Advanced Hybrid Integrated Transceivers to Realize Flexible Terabit Networking

P. Zakynthinos[1], G. Cincotti[2], M. Nazarathy[3], R. Kaiser[4], P. Bayvel[5], R. I. Killey[5], M. Angelou[6], S. B. Ezra[7], M. Irion[8], A. Tolmachev[3], B. Gomez Saavedra[4], J. Hoxha[2], V. Grundlehner[8], N. Psaila[9], G. Vollrath[10], R. Magri[11], G. Papastergiou[6] and I. Tomkos[1]

[1]Athens Information Technology Center, 19.5km Markopoulo Ave., Peania, Athens, 19002, Greece
[2]University Roma Tre, via Della Vasca Navale 84, Rome, I-00146, Italy
[3]Electrical Engineering Department, Technion, Israel Institute of Technology, Haifa, 32000, Israel
[4]Fraunhofer Heinrich Hertz Institute, Einsteinufer 37, 10587 Berlin, Germany
[5]Optical Networks Group, Department of Electronic and Electrical Engineering, University College London, Torrington Place, London WC1E 7JE, UK
[6]Optronics Technologies S.A., 79-81 Thessalonikis str, 18346 Moschato, Athens, Greece
[7]Finisar Corporation, Nes Ziona, Israel
[8]Albis Optoelectronics AG, Moosstrasse 2a, 8803 Rueschlikon, Switzerland
[9]Optoscribe Ltd, Suite 0/14, Alba Innovation Centre, Alba Campus, Livingston, West Lothian, UK
[10]Aifotec AG, Herpfer Straße 40, D-98617, Meiningen, Germany
[11]Ericsson Telecomunicazioni S.p.A., PDU Optical Networks - Systems & Technology - XOS/P, Via Moruzzi 1-CNR–Pisa, Italy

Abstract—Flexible optical networking has been introduced recently as a way to offer efficient utilization of the available optical resources. Flexible transceivers capable of generating and receiving tributaries with variable bandwidth characteristics are key subsystem elements for the realisation of a flexible optical networking system. This paper presents the main concept and developments envisioned by the EU funded project ASTRON, which targets the design, development and evaluation of a high-capacity, energy-efficient and bit-rate flexible optical transceiver capable of supporting rates from 10 Gb/s to beyond 1 Tb/s. The ASTRON technology relies on the combination of InP monolithic chips and Silica planar lightwave circuits to develop compact photonic integrated modules that exploit hybrid integration technologies.

I. Introduction

The emergence of bandwidth-consuming and highly dynamic services, dictates the evolution of old fixed optical networks that were based on wavelength division multiplexing (WDM). Traditional WDM-based networks offer the possibility to establish fixed connections (wavelengths) and bit rates, namely 10 Gb/s, 40 Gb/s, and recently 100 Gb/s, where the channels are modulated with a common (pre-defined) modulation format (e.g. On-Off Keying (OOK), Differential Phase Shift Keying (DPSK) or Quadrature Phase Shift Keying(QPSK)) and are spaced at a fixed channel spacing of 50 GHz. Flexibility in these networks is limited to that allowed by frequency-tunable lasers (i.e., each transponder can be assigned to a different wavelength) and to the limited reconfigurations allowed by optical switching nodes. As a result, the process of upgrading/modifying the network to adapt to changing traffic and network conditions is challenging. Additionally, there is a growing awareness that the bandwidth of deployed optical fiber is approaching its limit [1], termed capacity crunch. It is, thus, important, to maximise the use of scarce network resources - such as the fiber bandwidth—and to accommodate the ever-increasing and dynamic traffic demands.

Flexible optical networking concepts have attracted much discussion [2]. The term "flexibility" refers to the ability of the network to dynamically adjust its resources—such as the optical bandwidth and the modulation format—according to the requirements of each connection and/or service. Note that the terms "flexible", "flexgrid or flexigrid", "elastic", "tunable", and "gridless" are often used interchangeably in the literature. Recent advances in coherent optical orthogonal frequency division multiplexing (Co-OFDM) and Nyquist WDM (N-WDM) have set the stage for the design of flexible optical networks [3-4]. These technologies enable the formation of spectrally-efficient "super-channels", consisting of densely packed sub-channels, offering tunable bit-rates from a few tens of gigabits to the terabit per second range. Many elements are required to complete the "flexible optical networking puzzle", including the design

of new advanced network architectures and wavelength-routing algorithms and control plane). However, progress in the development in the design of flexible transceivers and switches is essential to enable the generation, switching, and reception of such super channels [5–7].

II. Flexible Transceivers

As traffic growth drives the demand for increasingly higher interface rates, research under this programme is focused on channels in the terabit per second range. To increase the total bit-rate, several options are open, including varying the symbol-rate, the modulation format etc. The deployment of higher order multi-level modulation formats leads to increased effective capacity and spectral efficiency—as a larger number of bits per symbol is transported. This improvement, however, results in reduced transparent transmission distance or reach. Similar trade-offs are observed when the symbol rate is increased. Due to technological limitations, such as the maximum sampling rate of analogue-to-digital and digital-to-analogue converters (ADCs/DACs), approaches that split up the targeted data rate into multiple parallel lower data rate streams have emerged. This leads us to the concept of super channels composed of multiple subcarriers. There are different approaches that enable the subcarriers to be efficiently aggregated: optical OFDM, N-WDM, and optical arbitrary waveform generation (OAWG). Optical OFDM uses orthogonal subcarriers with spacing equal to multiples of the inverse of the symbol period [2, 4]. N-WDM uses optical subcarriers with almost rectangular frequency spectrum, close or equal to the Nyquist limit for inter-symbol-interference free transmission, and these subcarriers are multiplexed with spacing close or equal to the symbol rate [3]. The ultimate spectral efficiency is almost identical for both methods under ideal conditions [8].

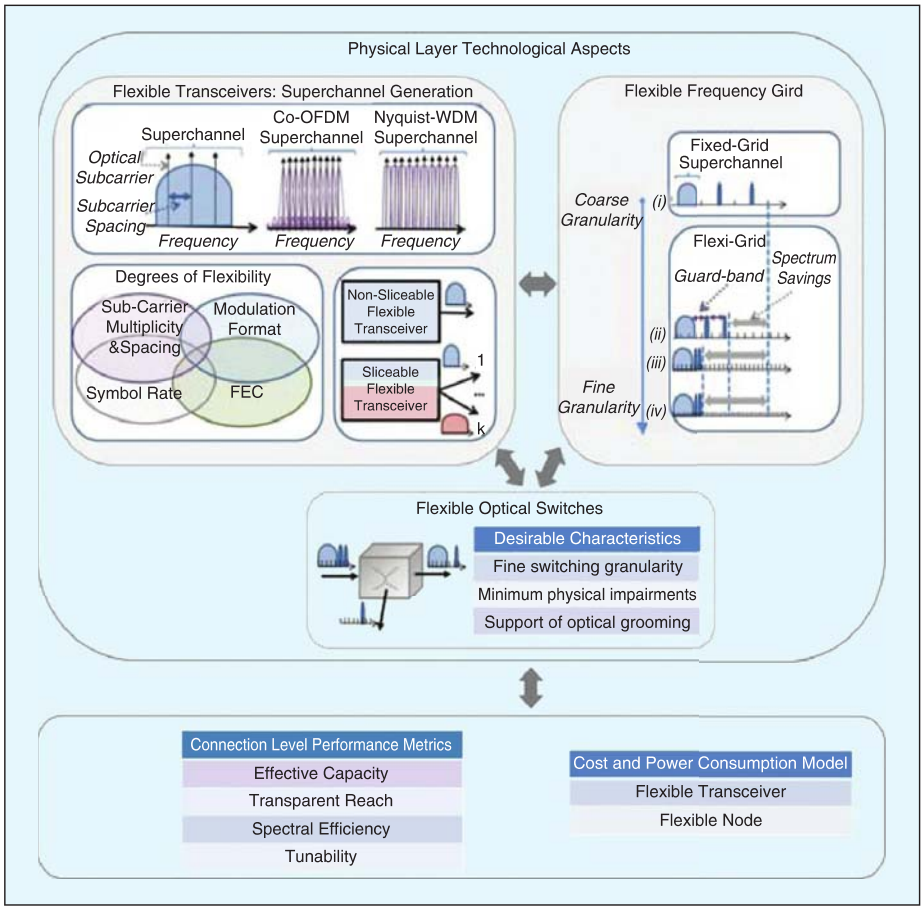

Figure 1. Physical layer concepts and solutions for flexible transceivers, flexible optical switches and the flexible frequency grid.

As shown in Fig. 1, different bandwidth available from flexible transceivers with respect to the modulation format, the symbol rate, the ratio of the forward error correction (FEC) and the payload, the number and the spacing of the subcarriers composing a super channel, as well as the inter-super channel spacing. Of course, not all degrees of flexibility need to be simultaneously available. Depending on the available degree of flexibility, different variants of flexible networking architectures can be defined. For example, in [9] the SLICE concept proposed that allows flexibility in the number of subcarriers, while in [10] a data-rate elastic optical network architecture is proposed that only allows single-carrier transmission technology. Another proposed architecture is the filterless optical network concept [11–12] where the active switching photonic devices are replaced with passive optical splitters and combiners. This architecture has been enabled by the recent transponder and digital signal breakthroughs offering a cost-effective and reliable network solution.

Increasing the available degree of flexibility, may improve the tunability of the transceiver at the expense of more complex and potentially cost-intensive transceiver design. Increasing the number of subcarriers, leads to linear increase in the effective capacity, but also decreases the maximum transparent reach—as the number of co-propagating channels increases. Additionally, the spectral efficiency is improved because the same inter-super channel guard band is assumed for a connection having greater effective capacity. Finally, increasing the spacing of the subcarriers within a super channel leads to increased reach—as the effect of inter-channel interference becomes less significant (however, note, that the effective capacity remains constant). Similar conclusions hold for the impact of the inter-super-channel spacing. Table 1 summarizes the effects of tuning various transceiver parameters.

While multiple options seem to be available from each of these potential degrees of freedom, this is not the case. It must be taken into account that it is not easy to have complete freedom in the adaptability of each of these degrees of flexibility as the complexity in the control of all these parameters and their values is quite difficult and their optimisation can be cost prohibitive or/and impractical. For example, the maximum transparent reach is obtained at the optimum launch power, which is a function of the symbol rate. It is a challenge to design transceivers to operate at different symbol rates within the same network. By setting a constant launch power for all cases, "penalties" are introduced in terms of the maximum transparent

Potential Degrees of Flexibility	Connection Level Metrics		
	Effective Capacity	Transparent Reach	Spectral Efficiency
Modulation Format	↑	↓	↑
Symbol Rate	↑	↓	↑
Ratio of FEC and Payload	↓	↑	↓
Number of Subcarriers	↑	↓	↑
Inter-Subcarrier Spacing within a Superchannel	–	↑	↓
Inter-Superchannel Spacing (Guard-band)	–	↑	↓

Table 1. The impact of the potential degrees of flexibility on the connection level metrics

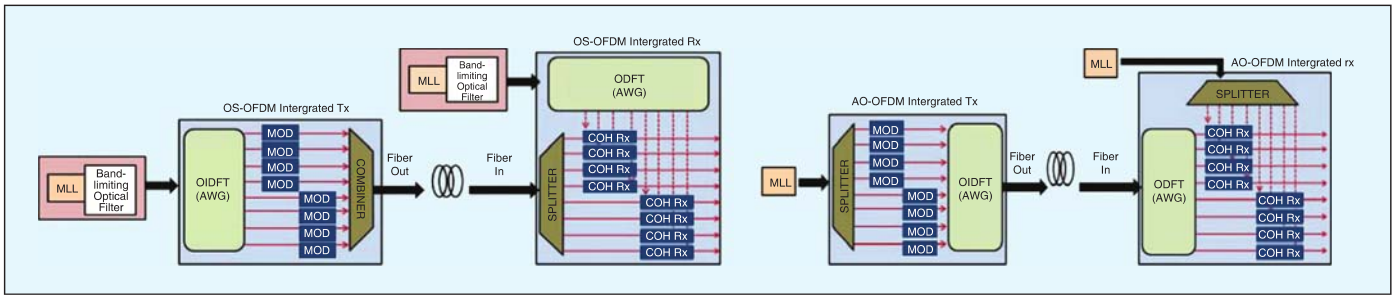

Figure 2. Left: Optically-Shaped OFDM (OS-OFDM) superchannel architecture, Right: AO-OFDM superchannel architecture

reach. On the other hand, by setting the optimum launch power for each case, the system design becomes impractical due to limitations at the amplification stages. This is addressed in [13], where trade-offs with respect to the utilized spectrum and the required transponders are identified. Defining the optimal combined settings of all of these different flexibility degrees is a complex optimization problem. Different combinations of these parameters imply different transceiver designs and, thus, different cost and power consumption characteristics.

III. The ASTRON Superchannel Architecture

The ASTRON researchers have explored the feasibility of generating OFDM-like ultra-broadband signals at the super-channel level and have concluded that an OFDM-like super-channel structure may be generated using two possible methods, appropriate for different applications:

1) The so-called all-optical OFDM (AO-OFDM) technique, generates OFDM sub-carriers all-optically [14–19] and is suited for access application [20–22], using both coherent and incoherent modulation formats. In the latter case, reduced or no digital signal processing (DSP) is needed, and the overall system power consumption is largely reduced.
2) For long-haul and metro applications the preferred method is what is elsewhere sometimes called "quasi-Nyquist coherent WDM" [23], which may be alternatively viewed as optically shaped OFDM (OS-OFDM).

Here, we briefly review the OS-OFDM and AO-OFDM architectures.

OS-OFDM architecture

The term shaped-OFDM [24–26] describes in the wireless literature a modification of conventional OFDM (which uses sub-carriers shaped in the frequency domain, such as (aliased) sinc functions) such that the sub-carrier spectral shapes are no longer sinc-like but are more confined in frequency, with lower overlap, such that the inter-sub-carrier interference is reduced. We point out here for the first time that a quasi-Nyquist coherent WDM" channel may be viewed precisely in these terms.

The OS-OFDM scheme shown in Fig. 2 (left), features a multi-port optical comb generator (MPORT-OCG) generating the OFDM CW un-modulated sub-carriers. The MPORT-OCG is implemented using a Mode-Locked-Laser (MLL), a band-limiting optical filter (BL-OF) and an optical inverse discrete Fourier transformer (OIDFT) device, realized by means of an integrated arrayed waveguide grating (AWG) device. The output ports of the MPORT-OCG optically feed an array of eight IQ modulators; these electro-optical modulators are driven by eight digital Nyquist transmitters equipped with a digital-to-analog converter (DAC), each generating 25 GHz quasi-Nyquist channels, each consisting of 15 Nyquist shaped single-carriers, jointly generated by means of DFT-Spread OFDM [26]. The modulator outputs are then passively combined in the combiner module to generate the Tx optical output.

At the receive side, each channel is optically selected by coherent detection and processed separately by means of a receiver structure with novel DSP. The local oscillator (LO) ports are derived as the outputs of another MPORT-OCG incorporated in the receiver, which would be matched to the one in the transmitter (reasonable frequency offsets between the two grids are corrected by the carrier recovery algorithms in the DSP). The performance of the OS-OFDM architecture was investigated using a MATLAB/Simulink platform and the simulation results are shown in Fig. 3 for QPSK and 16-QAM modulation formats.

The OS-OFDM transceiver structure is also able to support superchannels based on the Time/Frequency Packing technique

pioneered by Ericsson [28-29] where the 8 sub-carriers spaced 25 GHz are QPSK modulated at faster than Nyquist signaling rates up to 40 Gbaud. Spectral Efficiency higher than 5 bit/s/Hz can be achieved allowing for high capacity over ultra long haul distance performances with a low complexity modulation format.

AO-OFDM architecture

The AO-OFDM architecture shown in Fig. 2 (right) uses the same photonic components as building blocks to generate, transmit and receive the OFDM sub-channels. In a conventional AO-OFDM scheme, the MLL at the Tx has repetition rate equal to the channel spacing (e.g., 25 GHz), that coincides also with the baud-rate of each OFDM sub-channel. However, the ASTRON scheme allows additional bandwidth flexibility, since the baud rate can be suitably reduced to improve the system performances reducing the channel crosstalk, or increased to implement the so-called frequency-packing scheme [28–29], and enhance the system spectral efficiency.

The laser pulse stream is passively split to feed the IQ modulators in parallel, which are driven by eight electrical RF signals. We have experimentally verified that the AO-OFDM approach demands less bandwidth of optical modulators than the OS-OFDM scheme [16]. In a conventional AO-OFDM scheme, all the RF signals are synchronized and QAM-modulated; on the other hand, for access applications, it is possible to independently transmit eight RF channels, for an asynchronous multiple access. The eight modulator outputs are sent to the input ports of the passive AWG-based device that optically implements the DFT.

At the Rx, the same AWG-based performs the DFT and demultiplexes the OFDM sub-carriers. In access networks, where asynchronous access to shared media is the key feature, the sub-carriers are independently transmitted and received. It is worth nothing that the ASTRON AO-OFDM approach is identical to an optical code division multiple access (OCDMA) scheme [30], that has been demonstrated as an effective method to scale 10-Gbps-class optical access systems. Using the ASTRON AO-OFDM scheme, transmission distance over 100 km single-mode fiber without dispersion compensation have demonstrated, in a fully bandwidth flexible 10G (WDM)- and OCDM-based access system [31].

On the other hand, in a conventional AO-OFDM scheme, the eight RF signals are synchronously transmitted and received. In this case, we use a pulsed LO, i.e., the same MLL signal of the Tx, which is passively split to the eight 90° hybrids. Pulsed LO is equivalent to time gating, so that additional ultra-fast devices (e.g Electro-absorption modulators) are not required.

We have investigated the system performance of the scheme of Fig. 2 (right) by evaluating the BER as function of the overall optical power sent to the first fiber span of a compensated link, using Monte-Carlo simulations. From an inspection of Fig. 4(a), we observe that BER increases with the optical power, due to the nonlinear effects, that become dominant with respect to simplified spontaneous emission (ASE) noise by the optical amplifiers of the transmission link. Fig. 4(b) reports the maximum transmission distance versus the launched power for BER = 10^{-3}.

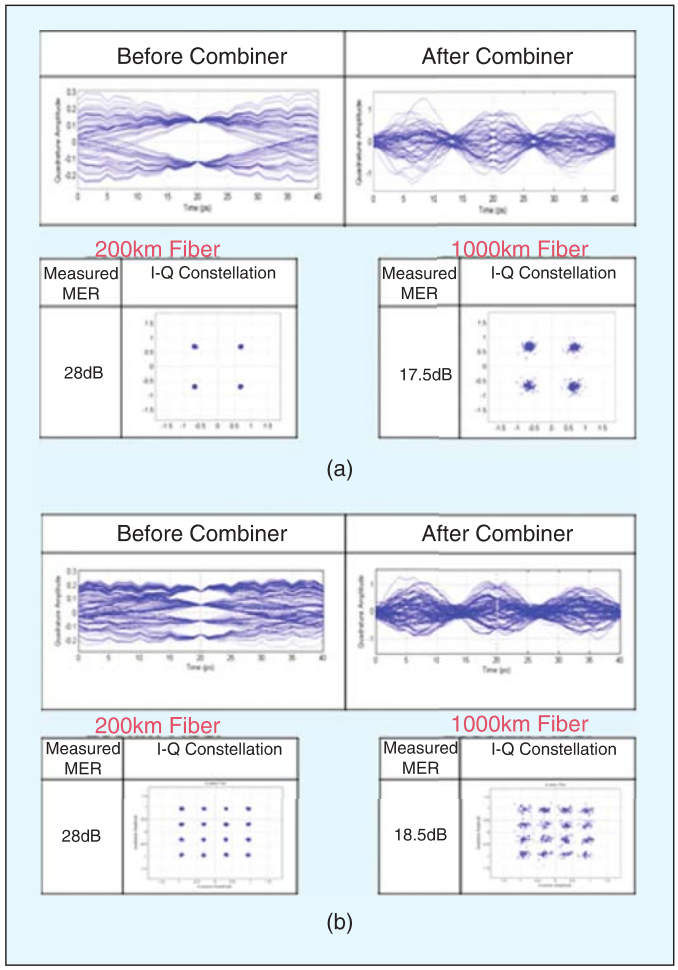

Figure 3. a) Top: Eye diagrams of individual channels before combiner and multiplexed all OS-OFDM subcarriers after combiner for QPSK modulation format. Bottom: Received constellation diagrams after 200 and 1000km of transmission b) Top: Eye diagrams of individual channels before combiner and multiplexed all OS-OFDM subcarriers after combiner for 16-QAM modulation format. Bottom: Received constellation diagrams after 200 and 1000 km transmission.

In the following two sections we briefly describe the photonic block developments towards the realisation of the complete ASTRON transceiver.

IV. The ASTRON Integrated Transmitter

The development and fabrication of the novel superchannel transmitter shown in Fig. 5 is based on the application and combination of a monolithic and a hybrid integration technology ("monolithic-on-hybrid"). However a full monolithic integration approach on InP would be the most attractive integration concept to provide such complex transmitter components in a compact design. But monolithic integration of such a large scale PIC is currently still a very ambitious and challenging task. For example, the expected large Tx PIC size and thus high optical loss, the limited InP substrate sizes, waste of valuable InP space to provide purely passive optical functions, optical and electrical RF crosstalk, heat management, and device yield are only a few issues in this context. Thus the monolithic-on-hybrid approach has been chosen for the transmitter fabrication in the ASTRON project.

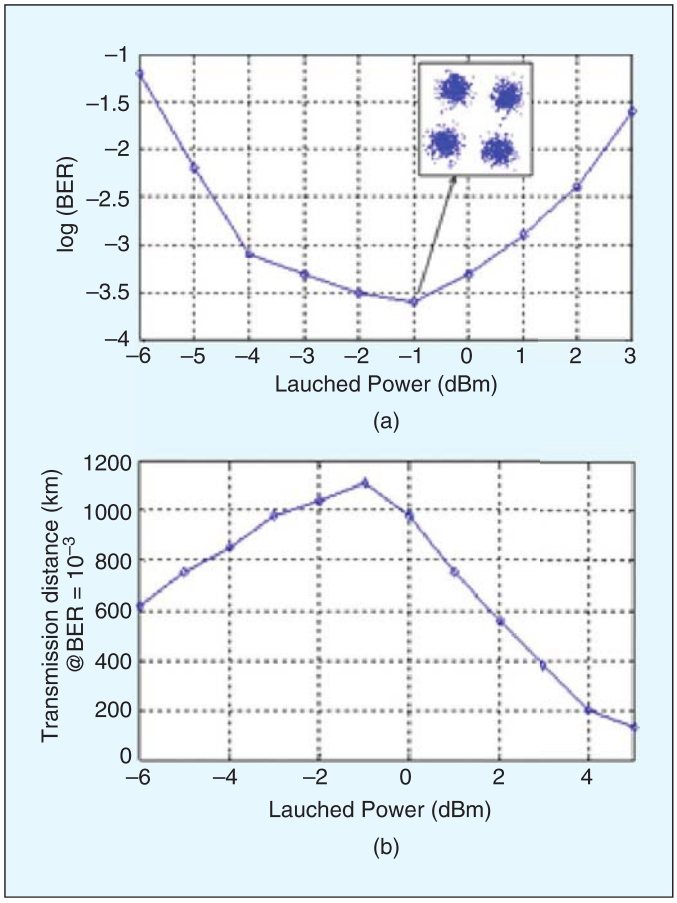

Figure 4. Simulation results for the AO-OFDM scheme considering a compensated transmission link of 800 km. a) BER versus launched power and b) Maximum transmission distance versus launched power.

The 8-channel ASTRON transmitter (Fig. 5) consists of a planar optical glass board and two InP-based 4-channel Mach-Zehnder modulator (MZM) IQ photonic integrated circuits (PIC). The board integrates all required passive optical waveguide elements for OFDM/NWDM super channel generation as well as all electrical RF/DC tracks to connect each IQ modulator on the board. The flip-chip ready MZM IQ PICs are mounted up-side down onto the planar glass board (Fig. 5) by using flip-chip bonding technology and by means of a solder process. To this aim precise pick-and-place techniques are used for hybrid chip assembly. The 4-channel MZM IQ PICs integrate periodically capacitive loaded series push-pull InP travelling wave electrode (TWE) MZ modulators as a basic building block [32-33] and high efficient GaInAs photodiodes for monitoring purposes and efficient setting of the IQ operating points.

In order to facilitate the hybrid assembly of the large InP MZM IQ PICs onto the glass motherboard, specific features are integrated on chip level (e.g. cleave initiators for precise chip cleaving, stand-off pillars for vertical waveguide alignment, and solder bump pads for flip-chip bonding).

On the glass board, a maskless 3D Ultrafast Laser Inscription (ULI) is used to fabricate the optical waveguides and all other passive devices (splitter/combiner, arrayed waveguide grating (AWG)). This process uses focused ultra-short laser pulses to induce a localized, permanent, sub-surface refractive index modification and subsequent waveguide structure. ULI has become a well-established technique for forming sub-surface waveguides in a range of materials. By exploiting nonlinear absorption, refractive index changes can be induced in three dimensions within a bulk substrate. Through careful control of the fabrication parameters, low loss 3D waveguides with a permanent isotropic increase in refractive index can be fabricated in standard optical glasses. Computer-controlled translation of a bulk substrate through the focus of the laser beam provides a flexible, software-defined fabrication process which is able to create and arbitrarily route waveguides in three dimensions as shown in Fig. 6.

The development and fabrication of such a novel and compact high capacity transmitter component has never been demonstrated before, either by using a full monolithic or by a monolithic-on-hybrid approach. Thus the transmitter development and assessment in ASTRON represents also a first general proof regarding a possible commercial application of this technology.

V. The ASTRON Integrated Coherent Receiver

In recent years, numerous examples of multichannel integrated receiver modules have appeared that rely on hybridisation of active components onto passive waveguides. Coherent modules typically consist of two arms, having two 90° hybrids that feed a total of 4 balanced photodiode pairs. Furthermore, for both coherent and non-coherent applications, the throughput of these state-of-the-art, highly integrated multi-channel receivers typically ranges up to 100 Gb/s.

The ASTRON project brings that figure beyond 1 Tb/s, which causes a substantial increase in component count and receiver module complexity. The integrated coherent receiver consists of a planar silica receiver motherboard that integrates an 8 × 8 Arrayed Waveguide Grating (AWG) based structure able to perform the DFT on incoming super-channels, an integrated optical coupler,

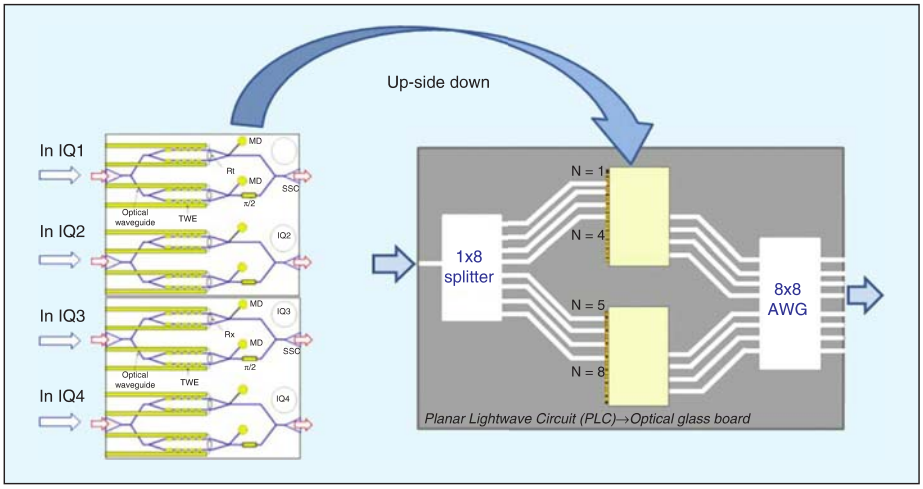

Figure 5. Schematic of the ASTRON transmitter integrated board. Two flip-chip ready InP-based 4-channel MZM IQ PICs (left) are assembled onto the glass board by utilizing flip-chip bonding technology.

eight 90° optical hybrids and a large number of high speed InP-based, balanced photodiode arrays with low intra-channel optical cross-talk, that can be hybridized to the silica motherboard with very efficient optical coupling. Moreover 45° mirrors for optimum optical board-to-chip coupling to the high speed InP photodiodes as well as all required electrical RF connections and transmission lines are fabricated on the glass motherboard.

The InP chips are twin arrays of balanced, ultra high-speed photodiodes with an active diameter of 24 µm. These photodiodes are optimized to handle data rates of over 25 Gb/s with a low bias voltage of 2 V as shown in Fig. 7. The developed high speed photodiodes feature monolithically integrated backside lenses that greatly facilitate the optical coupling and ensure a low loss optical path. In these chips the area with maximum responsivity is about a factor of three larger for the photodiode with integrated backside lens compared to a photodiode with a conventional flat entry, which gives a significant advantage in terms of optical alignment.

The hybrid assembly of the photodiode chips onto the silica Rx motherboard is performed by a solder process. Therefore the chips feature alignment marks and contact pads on the chip topside and solderable support pads on the backside. The hybrid assembly through a soldering process requires a precise handling of the photodiode to place it with the necessary accuracy onto the destination platform. Therefore a pick-up tool with the appropriate size to fit to the geometry of the photodiode is used. The photodiodes are assembled onto the motherboard with the lens side facing down. The light out of the board silica waveguides is coupled into the photodiode lens with a monolithic 45° mirror structure. The light beam is focused by photodiode the lens, travels through the transparent substrate and reaches the photodiode active area where it is effectively absorbed and converted into an electrical current. Besides the mirror structures, all passive structures (e.g. optical waveguides, optical splitter, AWG, 900 hybrids) are fabricated using the same 3D laser inscription described in the previous section.

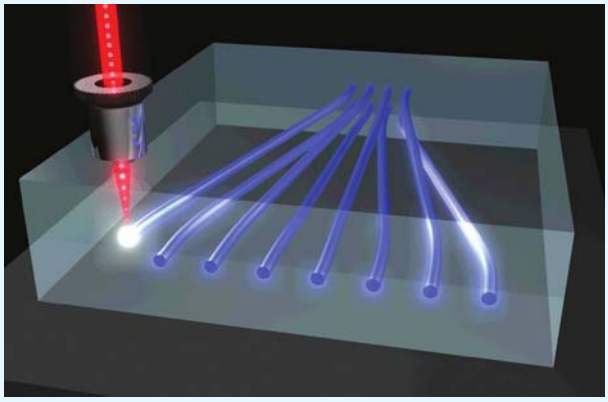

Figure 6. Maskless 3D waveguide fabrication using ultrafast laser irradiation with tightly focused beam.

VI. Digital Signal Processing

Software defined optical transceivers offer flexibility in channel coding, modulation, and the number of subcarriers per wavelength. Modulation format and coding levels are flexible and controlled by software; adjusting the number of bits per symbol, choosing the right modulation format and optimising the filter bandwidths allows throughput to be maximized for a given set of link parameters, including link length, amplifier noise figures, dispersion and fibre nonlinearity. Reprogrammable DSP allows optimum network utilization [34] with respect to applications, channel requirements and quality of service. For example, the signal bandwidth can be varied, enabling networks based on flexible WDM grids, and allowing more efficient use of resources.

To enable future ultra-high capacity flexible networks, one major objective is to extend the transmission reach and spectral efficiency of OFDM super-channels well beyond the state-of-the-art by digitally mitigating all optical channel impairments. Sub-banded DSP with under-decimated filter banks is a recent DSP HW architecture whereby the bandwidth of the optical channel is digitally partitioned into multiple spectrally disjoint sub-bands to be processed in parallel [35-37]. The resulting optical receiver ASICs are applicable to long-haul and metro photonic communication and may provide substantial energy efficiency savings of 30%-50% in the power consumption of the DSP section. Moreover, as the processing is structured in multiple independent sub-bands (e.g. for a channel of 25 GHz, 15 sub-bands of ~1.7 GHz each), the performance of the multiple parallel sub-band receivers exceeds that of a reference full band 25 GHz conventional Rx which processes the full 25 GHz wide spectrum at once. In ASTRON we have conceived [35] a twice under-decimated filter bank DSP structure enabling the partitioning into multiple sub-band with high computational efficiency.

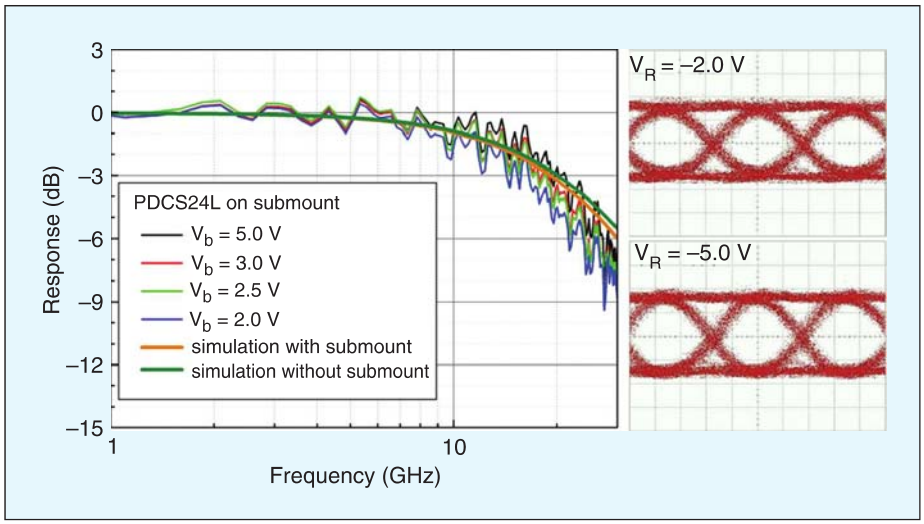

Figure 7. Left: Photodiode chips frequency response measurements for different bias voltages. A 3-dB bandwidth of over 20 GHz for a low bias voltage of –2 V is achieved. Right: Eye diagrams at at a bit rate of 28 Gb/s for applied bias voltages of –2 V and –5 V.

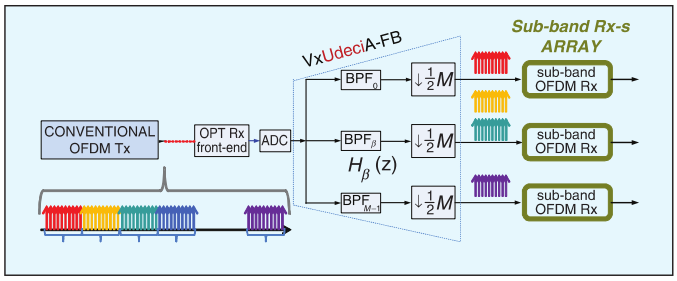

Figure 8. Novel sub-banded reception in an OFDM link using a conventional OFDM

We briefly address the root causes of sub-banded performance improvement and the resulting improved characteristics of adaptive acquisition and tracking under the sub-banded paradigm. In terms of DSP hardware architecture, digital sub-banding amounts to an alternative mode of parallelizing the signal processing task to multiple slower processors, whereby the parallelization is performed in the frequency-domain (FD) rather than in the time-domain (TD). FD parallelization of the DSP processing is especially suited to the long-haul optical fiber channel, the reason being that chromatic dispersion grows with bandwidth squared and polarization mode dispersion (PMD) also increases with bandwidth, hence our "divide&conquer" approach, partitioning the processing into multiple frequency-domain sub-bands, radically simplifies the filters length, hence real-time computational load is reduced.

Sub-banding should further improve robustness and adaptability in the "control path". In a full-band Rx, channel estimation and adaptive tracking generally take a major toll on overall complexity and performance. Sub-banding features the frequency-flat sub-banding advantage, attaining rapid and accurate convergence, yielding fast optical channel acquisition and tracking. The resulting receiver ASICs are a factor of approximately two less complex in their DSP section in comparison to conventional receiver ASICs. Additional useful strategies enabled by the sub-banding paradigm are: (i): sleep-mode selectively turning sub-bands on and off for energy-efficiency. (ii): Software defined transceivers over flexi-grid variable-channel formation by aggregating sub-bands even across channel boundaries. (iii): Efficient photonic switching at the physical layer, based on digital cross-connects with high-granularity (down to sub-bands) for highly efficient networking. (iv): the potential for sub-banded spatial-division multiplexing equalization.

VII. Impact

The ASTRON transceiver architecture relies on leading edge technology providing important contributions beyond the state-of-the-art with respect to photonic technologies, yet it also provides a favorable ground for future technologies on the future network as a whole. The project aspires to contribute to communications networks by increasing the transparency, the information throughput, and the power consumption reduction in adaptive Tb/s networks. In addition to the inherent technological benefits, designing and developing compact and scalable adaptive software-defined transceivers provides telecom operators with the cost-effectiveness required to ensure rapid uptake by the industry. In such context, the ASTRON developed devices assume a role as key enablers for the next generation core, metro and access infrastructures. Besides, the project provides the complete path to turn its innovative research into a high-value photonic integrated product, reinforcing EU's position in the field. The great involvement of industry in the project gives a good insight into the marketing leverage and commercial potential of ASTRON.

Acknowledgements

The ASTRON project is funded by the EU Seventh Framework Programme (FP7/2007-2013) under grant agreement n° 318714.

References

[1] R. Essiambre, G. Kramer, P. Winzer, G. Foschini, and B. Goebel, "Capacity limits of optical fiber networks," Lightwave Technology, Journal of, vol. 28, no. 4, pp. 662–701, 2010.

[2] O. Gerstel, M. Jinno, A. Lord, and S. J. B. Yoo, "Elastic optical networking: a new dawn for the optical layer?" Communications Magazine, IEEE, vol. 50, no. 2, pp. s12–s20, 2012.

[3] G. Bosco, V. Curri, A. Carena, P. Poggiolini, and F. Forghieri, "On the performance of Nyquist-WDM terabit superchannels based on PMBPSK, PM-QPSK, PM-8QAM or PM-16QAM subcarriers," Lightwave Technology, Journal of, vol. 29, no. 1, pp. 53–61, 2011.

[4] G. Zhang, M. De Leenheer, A. Morea, and B. Mukherjee, "A survey on OFDM-based elastic core optical networking," Communications. Surveys Tutorials, IEEE, vol. 15, no. 1, pp. 65–87, 2013.

[5] H. Takara, T. Goh, K. Shibahara, K. Yonenaga, S. Kawai, and M. Jinno, "Experimental demonstration of 400 Gb/s multi-flow, multi-rate, multireach optical transmitter for efficient elastic spectral routing," in 37th European Conference and Exhibition on Optical Communication (ECOC), 2011.

[6] X. Liu, S. Chandrasekhar, X. Chen, P. Winzer, Y. Pan, B. Zhu, T. Taunay, M. Fishteyn, M. Yan, J. Fini, E. Monberg, and F. Dimarcello, "1.12-Tb/s 32-QAM-OFDM superchannel with 8.6-b/s/Hz intrachannel spectral efficiency and space-division multiplexing with 60-b/s/Hz aggregate spectral efficiency," in Optical Communication (ECOC), 2011 37th European Conference and Exhibition on, 2011.

[7] E. Ip, P. Ji, E. Mateo, Y.-K. Huang, L. Xu, D. Qian, N. Bai, and T. Wang, "100G and beyond transmission technologies for evolving optical networks and relevant physical-layer issues," Proceedings of the IEEE, vol. 100, no. 5, pp. 1065–1078, 2012.

[8] G. Bosco, A. Carena, V. Curri, P. Poggiolini, and F. Forghieri, "Performance limits of Nyquist-WDM and CO-OFDM in high-speed PMQPSK systems," Photonics Technology Letters, IEEE, vol. 22, no. 15, pp. 1129–1131, 2010.

[9] M. Jinno, H. Takara, B. Kozicki, Y. Tsukishima, T. Yoshimatsu, T. Kobayashi, Y. Miyamoto, K. Yonenaga, A. Takada, O. Ishida, and S. Matsuoka, "Demonstration of novel spectrum-efficient elastic optical path network with

per-channel variable capacity of 40 Gb/s to over 400Gb/s," in Optical Communication, 2008. ECOC 2008. 34th European Conference on, 2008.

[10] O. Rival and A. Morea, "Elastic optical networks with 25-100G format-versatile WDM transmission systems," in OptoeElectronics and Communications Conference (OECC), 2010 15th, 2010.

[11] Guillaume Mantelet, Andrew Cassidy, Christine Tremblay, David V. Plant, Paul Littlewood, and Michel P. Bélanger, "Establishment of Dynamic Lightpaths in Filterless Optical Networks", Journal of Optical Communications and Networking, Vol. 5, Issue 9, pp. 1057–1065 (2013).

[12] Émile Archambault, Daniel O'Brien, Christine Tremblay, François Gagnon, Michel P. Bélanger, and Éric Bernier, "Design and Simulation of Filterless Optical Networks: Problem Definition and Performance Evaluation.

[13] E. Palkopoulou, G. Bosco, A. Carena, D. Klonidis, P. Poggiolini, and I. Tomkos, "Network performance evaluation for nyquist-WDM-based flexible optical networking," in European Conference and Exhibition on Optical Communication., 2012, p. Mo.1.D.2.

[14] Zhenxing Wang, Konstantin S. Kravtsov, Yue-Kai Huang, and Paul R. Prucnal, "Optical FFT/IFFT circuit realization using arrayed waveguide gratings and the applications in all-optical OFDM system," Opt. Express 19, 4501-4512 4501-4512 (2011).

[15] S. Shimizu, N. Wada, G. Cincotti, "Demonstration of a 8x12.5 Gbit/s all-optical OFDM system with an arrayed waveguide grating and waveform reshaper," European Conference on Optical Communication (ECOC), Amsterdam, The Netherlands 2012.

[16] Arthur James Lowery and Liang Du, "All-optical OFDM transmitter design using AWGRs and low-bandwidth modulators," Opt. Express 19, 15696–15704 (2011).

[17] K. Lee, C. T. D. Thai, and J.-K. K. Rhee, "All optical discrete Fourier transform processor for 100 Gbps OFDM transmission," Opt. Express 16(6), 4023–4028 (2008).

[18] Y.-K. Huang, D. Qian, R. E. Saperstein, P. N. Ji, N. Cvijetic, L. Xu, and T. Wang, "Dual-polarization 2×2 IFFT/FFT optical signal processing for 100-Gb/s QPSK-PDM all-optical OFDM," in Conference on Optical Fibre Communication (OFC) (Optical Society of America, San Diego, CA, 2009), paper OTuM4.

[19] D. Hillerkuss, *et al.* "Simple all-optical FFT scheme enabling Tbit/s real-time signal processing," Optics Express 18, pp. 9324–9340 (2010).

[20] J. Hoxha, G. Cincotti, N. Diamantopoulos, P. Zakynthinos, I. Tomkos, "All-optical implementation of OFDM/NWDM Tx/Rx," invited paper International Conference on Optical Transparent Networks (ICTON) Cartagena, Spain 2013.

[21] S. Shimizu, G. Cincotti, N. Wada, "Demonstration and performance investigation of all-optical OFDM systems based on arrayed waveguide gratings," Optics Express, 20, B525-B534 (2012) http://www.opticsinfobase.org/oe/abstract.cfm?uri=oe-20-26-B525.

[22] L. B. Du, J. Schröder, M. M. Morshed, B. J. Eggleton, A. J. Lowery, "Optical inverse Fourier transform generated 11.2-Tbit/s no-guard-interval all-optical OFDM transmission," Optical Fiber Conference (OFC), OW3B.5, Anaheim, California 2013.

[23] Q. Yang, N. Kaneda, X. Liu, S. Chen, W. Shieh, and Y. K. Chen, "Digital Signal Processing for Multi-gigabit Real-time OFDM," in Signal Processing in Photonic Communications (SPPCom'11), Advanced Photonics OSA Conference, 2011, vol. 1, no. c, p. SPMB2.

[24] J. Du and S. Signell, "Classic OFDM Systems and pulse shaping OFDM / OQAM Systems, KTH - Royal Institute of Technology report," 2007.

[25] D. Vuletic, W. Lowdermilk, and F. Harris, "Advantage and Implementation Considerations of Shaped OFDM Signals," in Signals, Systems and Computers, Thirty-Seventh Asilomar Conference, 2003, pp. 683–687.

[26] Y. Tang, W. Shieh, and B. S. Krongold, "DFT-Spread OFDM for Fiber Nonlinearity Mitigation," IEEE Photon. Technol. Lett., vol. 22, no. 16, pp. 1250–1252, Aug. 2010.

[27] G. Cincotti, "What else can an AWG do?", Optics Express, Volume 20, Issue 26, Page B288, Dec. 2012.

[28] L. Poti et al. "Casting 1 Tb/s DP-QPSK Communication into 200 GHz Bandwidth," ECOC 2012.

[29] F. Cavaliere, L. Giorgi and R. Sabella, "Overcoming the challenges of very high-speed optical transmission," Ericsson Review, Oct 2013.

[30] X. Wang, N. Wada, N. Kataoka, T. Miyazaki, G. Cincotti and K.-i. Kitayama, '100 km field trial of 1.24 Tbit/s, spectral efficient, asynchronous 5 WDM X 25 DPSK-OCDMA using one set of 50×50 ports large scale en/decoder,' postdeadline paper Optical Fibre Communication Conference OFC, Anaheim, California 2007.

[31] T. Kodama, Y. Tanaka, S. Yoshima, N. Kataoka, J.-i. Nakagawa, S. Shimizu, N. Wada, and K.-i. Kitayama, "Scaling the system capacity and reach of a 10G-TDM–OCDM-PON system without an en/decoder at an ONU J. Optical Communication Networks, vol. 5, pp. 134–143, 2013.

[32] K. Prosyk et al.: Travelling wave Mach-Zehnder modulators, 25th International Conf. on Indium Phosphide and Related Materials (IPRM), 2013, Kobe (Japan), paper M03-1.

[33] K.O. Velthaus, et al: High performance InP-based Mach-Zehnder modulators for 10 to 100 Gb/s optical fiber transmission systems, in Proc. of IPRM 2011, Berlin (Germany), April 2011, paper #Th9.2.1.

[34] C. Glingener, 'Optical networking trends and evolution', in Proc. OFC 2011, Paper OThAA1.

[35] M. Nazarathy and A. Tolmachev, "Sub-banded DSP architectures based on under-decimated filter-banks for coherent OFDM receivers," IEEE Signal Process. Mag., no. Special Issue on Advanced DSP and Coding for Multi-Tb/s Optical Transport, 2014.

[36] A. Tolmachev and M. Nazarathy, "Filter-bank based efficient transmission of Reduced-Guard-Interval OFDM," Opt. Express, vol. 19, no. 26, pp. 370–384, 2011.

[37] K.-P. Ho, "Subband equaliser for chromatic dispersion of optical fibre," Electron. Lett., vol. 45, no. 24, p. 1224, 2009.